Antiferromagnetic ordering in the novel Ho_3Ge_4 and $HoGe_{1.5}$ compounds studied by neutron diffraction and magnetic measurements

1998 J. Phys.: Condens. Matter 10 2881

(http://iopscience.iop.org/0953-8984/10/13/007)

J. Phys.: Condens. Matter **10** (1998) 2881–2891. Printed in the UK PII: S0953-8984(98)89428-9

Antiferromagnetic ordering in the novel Ho_3Ge_4 and $HoGe_{1.5}$ compounds studied by neutron diffraction and magnetic measurements

O Zaharko†‖, P Schobinger-Papamantellos†, C Ritter‡, Y Janssen§, E Brück§, F R de Boer§ and K H J Buschow§

† Laboratorium für Kristallographie, ETHZ, CH-8092 Zürich, Switzerland
‡ Institut Laue–Langevin, 156X, 38042 Grenoble Cédex, France
§ Van der Waals–Zeeman Institute, University of Amsterdam, 1018 XE Amsterdam, The Netherlands

Received 21 November 1997

Abstract. The magnetic ordering of the novel binary compounds Ho_3Ge_4 (Er_3Ge_4 structure type, space group *Cmcm*) and $HoGe_{1.5}$ (AlB_2 structure type, space group $P6/mmm$) has been studied by neutron diffraction and magnetic measurements. Antiferromagnetic ordering of Ho_3Ge_4 sets in below $T_N = 12$ K. The two Ho sites order independently with two distinct order parameters associated with the same wave vector $\boldsymbol{q} = (010)$. Both sublattices have a uniaxial antiferromagnetic moment arrangement but with mutually perpendicular orientations. In a first step ($T < T_N$) the Ho_1 sublattice orders with a uniaxial moment arrangement along $\boldsymbol{c}$. In a second step ($T < T_1 = 6.6$ K) the Ho_2 sublattice orders perpendicular to Ho_1 with a uniaxial arrangement along $\boldsymbol{a}$. Below T_1 the resulting two-dimensional canted antiferro-magnetic structure is described by the monoclinic magnetic space group $Cp11\frac{2_1}{m'}i'(\mathrm{Sh}_{14}^{82})$. At 1.4 K the ordered moment values of Ho_1 and Ho_2 are 8.9(1) μ_B/atom and 7.2(2) μ_B/atom, respectively.

The magnetic ordering of the coexisting novel phase $HoGe_{1.5}$ with the AlB_2 structure type (space group $P6/mmm$) has been also studied. The Ho moments order antiferromagnetically below $T_N = 10$ K. The collinear moment arrangement is associated with the wave vector ($\boldsymbol{q} = 001/2$) and is described by the magnetic space group $P_{2c}11\frac{2'}{m'}(\mathrm{Sh}_{11}^{56})$. At 1.4 K the ordered magnetic moment $\mu_{Ho} = 6.2(6)$ μ_B is confined to the (001) plane.

1. Introduction

The magnetic ordering in several R_3Ge_4 compounds (R = Tb, Dy, Er) with the Er_3Ge_4 structure was recently studied [1–3] by powder neutron diffraction and magnetic measurements. The orthorhombic Er_3Ge_4 structure (space group *Cmcm*) possesses two rare earth sites, R_1 at 8(f) and R_2 at 4(c) and three Ge sites [4]. The R atoms form trigonal prisms centred by Ge atoms and are stacked along the $\boldsymbol{a}$ axis. Within the $(0yz)$ plane adjacent prisms along $\boldsymbol{b}$ or $\boldsymbol{c}$ are shifted by $x = 1/2$. This geometric arrangement results in nearest-neighbour R–R interactions arrayed on a triangle and leads to magnetic frustration and complex ordering types.

The magnetic order in rare-earth compounds arises as a result of competing exchange interactions and important anisotropy induced by the crystal field interaction.

‖ On leave from the Institute of Inorganic Chemistry, Lviv State University, Lviv, Ukraine.

0953-8984/98/132881+11$19.50

In Er_3Ge_4 [1] the two Er sites order simultaneously below $T_N = 7.3$ K with a triangular antiferromagnetic moment arrangement within the $(0yz)$ plane. Adjacent prisms display different chiralities. The Er_2 moment direction lies along the $\boldsymbol{c}$-axis over the whole magnetically ordered T-interval while a reorientation of the Er_1 moments within the $(0yz)$ plane sets in at 4 K.

Dy_3Ge_4 [2] displays a two-step antiferromagnetic ordering below $T_N = 19$ K. The Dy_1 moments order below $T_N = 19$ K with their moment directions along the $\boldsymbol{a}$-axis while the Dy_2 moments order below $T_i = 6$ K with their moment directions along the $\boldsymbol{c}$-axis. The two Dy sites order independently with two distinct order parameters. Each sublattice has a uniaxial antiferromagnetic moment arrangement but the corresponding moment orientations are mutually perpendicular.

Tb_3Ge_4 [3] orders antiferromagnetically in two steps below $T_N = 28$ K. In a first step the Tb_1 sublattice orders with a collinear moment arrangement along $\boldsymbol{a}$ which persists down to $T_1 = 16.5$ K. Below T_1 a reorientation of the Tb_1 moments takes place. Simultaneously the Tb_2 moments order with a collinear arrangement along $\boldsymbol{c}$.

We report in this paper on the magnetic ordering of the Ho_3Ge_4 compound and we will discuss our results in the light of similar ordering phenomena observed previously in other compounds of the same structure type.

2. Sample preparation

The polycrystalline sample of composition Ho_3Ge_4 was prepared by arc melting of the elements in an atmosphere of purified argon gas. The purity of the starting materials was 99.9% for Ho and 99.99% for Ge. After arc melting the sample was vacuum annealed at 800 °C for three weeks and subsequently quenched in water. As is shown in the next sections the presence of secondary phases (mainly $HoGe_{1.5}$) was detected. However, due to the peritectoid way of formation of Ho_3Ge_4 we did not succeed in preparing a single-phase sample in repeated trials.

3. Specific heat and magnetic measurements

Magnetic measurements were made with a SQUID magnetometer. The temperature dependence of the reciprocal susceptibility is shown in figure 1. Curie–Weiss behaviour is followed down to about 10 K. From the slope and the intercept with the horizontal axis we derive the values $\mu_{eff} = 11.0\ \mu_B$/Ho and $\theta_P = -6.4$ K for the effective moment and the asymptotic Curie temperature, respectively. The former value is close to the free ion value (10.6 μ_B/Ho). The temperature dependence of the magnetization, also shown in figure 1, is characterized by an antiferromagnetic type transition at about 11 K.

Results of specific heat measurements made on Ho_3Ge_4 are shown in figure 2. The low-temperature behaviour is shown in more detail in the inset. There are two distinct magnetic phase transitions at 11.4 K and 6.6 K. Anticipating the detailed neutron diffraction study of the thermal behaviour of the magnetic intensities presented below, magnetic ordering of the two Ho sublattices occurs in two steps. The Ho_1 moments order below $T_N = 12$ K, but magnetic ordering of the moments at the Ho_2 site occurs at much lower temperatures, below $T_1 = 6.6$ K. This two-step ordering is clearly visible in the specific-heat data shown in figure 2. The upturn of the specific heat at the lowest temperatures is attributed to nuclear contributions of the Ho atoms.

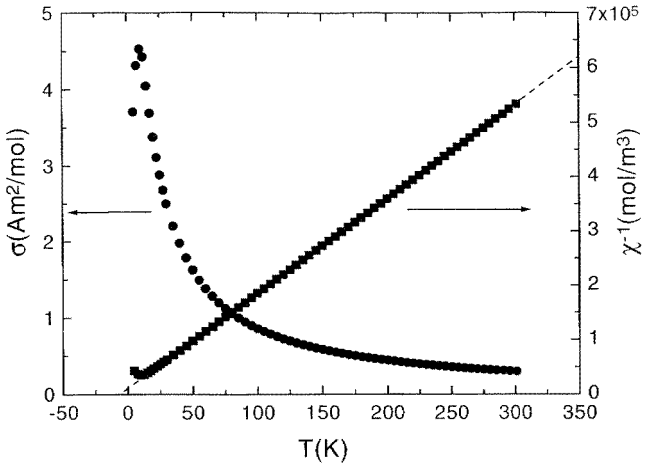

Figure 1. Temperature dependence of magnetization of Ho_3Ge_4 measured in a field of 0.2 T (left scale) and temperature dependence of the reciprocal susceptibility (right scale). The units are expressed per mol Ho_3Ge_4.

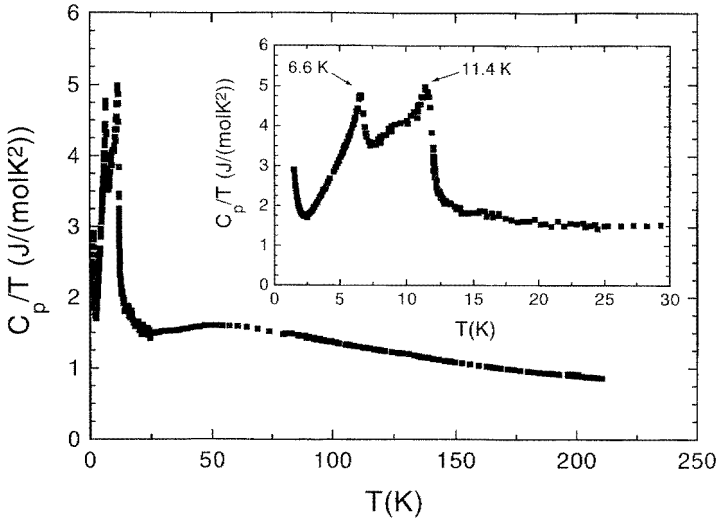

Figure 2. Temperature dependence of the specific heat C_p/T of Ho_3Ge_4. The inset shows the low-temperature data in an expanded temperature scale. The units are expressed per mol Ho_3Ge_4.

4. Neutron diffraction

Neutron diffraction experiments were carried out at the facilities of the ILL reactor (Grenoble) D1B diffractometer ($\lambda = 2.52$ Å). The data were collected in the temperature range 1.4–125 K; the step increment in 2θ was 0.2°. The data analysis was performed with the Fullprof program [5].

4.1. Crystal structure of Ho_3Ge_4

The neutron diffraction patterns in the paramagnetic state confirm the crystal structure of Ho_3Ge_4 as reported in [4]. Results of the 38.4 K refinement are displayed in figure 3(a) and in table 1. The refinement comprises the coexisting secondary phases (see section 4.5) and there is good agreement between the experimental and the calculated patterns ($R_n = 5.3\%$).

Table 1. Refined parameters from neutron diffraction data of Ho_3Ge_4 (space group *Cmcm*): (a) at 38.4 K (paramagnetic state), (b) at 10.7 K in the magnetically ordered HT region (magnetic space group $Cp\frac{222_1}{m'c'm}i'(\mathrm{Sh}_{52}^{318})$), (c) at 1.4 K in the magnetically ordered LT region (magnetic space group $Cp11\frac{2_1}{m'}i'(\mathrm{Sh}_{11}^{56})$) and of $HoGe_{1.5}$ (space group $P6/mmm$, magnetic space group $P_{2c}11\frac{2'}{m'}(\mathrm{Sh}_{11}^{56})$).

	38.4 K		10.7 K		1.4 K	
	y	*z*	*y*	*z*	*y*	*z*
Ho_3Ge_4						
Ho_1 8f: (0, *y*, *z*)	0.329(1)	0.097(1)	0.3305(7)	0.098(9)	0.3323(8)	0.097(3)
Ho_2 4c: (0, *y*, 1/4)	0.053(3)	0.25	0.053(3)	0.25	0.044(2)	0.25
Ge_1 8f: (0, *y*, *z*)	0.373(2)	0.889(1)	0.375(2)	0.889(1)	0.381(3)	0.889(2)
Ge_2 4c: (0, *y*, 1/4)	0.773(2)	0.25	0.772(2)	0.25	0.771(4)	0.25
Ge_3 4a: (0, 0, 0)	0.0	0.0	0.0	0.0	0.0	0.0
μ_{1z} [μ_B], μ_{2x} [μ_B]			5.73(6)	—	8.9(1)	7.2(2)
a, *b*, *c* [Å]	4.0085(8), 10.550(2), 14.132(3)		4.0049(5), 10.541(2), 14.110(2)		4.0055(6), 10.543(2), 14.105(3)	
R_n%, R_m%	5.3, —		5.8, 6.0		5.2, 5.2	
R_{wp}%, R_{exp}%	12.2, 4.7		12.2, 3.6		13.2, 2.0	
$HoGe_{1.5}$						
Ho 1a: (0, 0, 0) μ_x [μ_B]					6.2(6)	
Ge 2d: (1/3, 2/3, 1/2)						
a, *c* [Å]	3.8985(8)	4.097(1)	3.8952(7)	4.092(1)	3.895(1)	4.0939(3)
R_n%, R_m%	5.7, —		3.1, —		7.3, 6.1	

4.2. The magnetic ordering of Ho_3Ge_4 in the range T_1–T_N

Below $T_N = 12$ K a large number of magnetic reflections appear at reciprocal lattice positions that do not obey the C-centring condition of Ho_3Ge_4 and lead to the anticentred magnetic C_P lattice with the wave vector $\boldsymbol{q} = (010)$. Similar to all other studied R_3Ge_4 compounds, the intensity of the (011) magnetic line is dominant (figure 3(b), (c)). However, the topology and the relative intensities of the other magnetic reflections differ from those of the other studied compounds.

The refinement of the 10.7 K pattern leads to a uniaxial magnetic moment arrangement of only the Ho_1 site 8(f), the moments pointing along the $\boldsymbol{c}$-axis. The arrangement of the Ho_1 moments ((1): $(0, y, z)$, (2): $(0, -y, 1/2 + z)$, (3): $(0, y, 1/2 - z)$, (4): $(0, -y, -z)) + (1/2, 1/2, 0)$) is described by the mode C_z–C_z $(+ + - - - - ++)$ in the notation of [6]. From the eight magnetic space groups associated with the *Cmcm* space group and the wave vector $\boldsymbol{q} = (010)$ (see table 2 in [2]) only $Cp\frac{222_1}{m'c'm'}i'(\mathrm{Sh}_{52}^{318})$ is compatible with this mode. The low reliability factors $R_n = 5.8\%$, $R_m = 6.0\%$ and the concomitant small difference between the experimental and the calculated intensities at 10.7 K confirm the correctness of the model (figure 1(b), table 1).

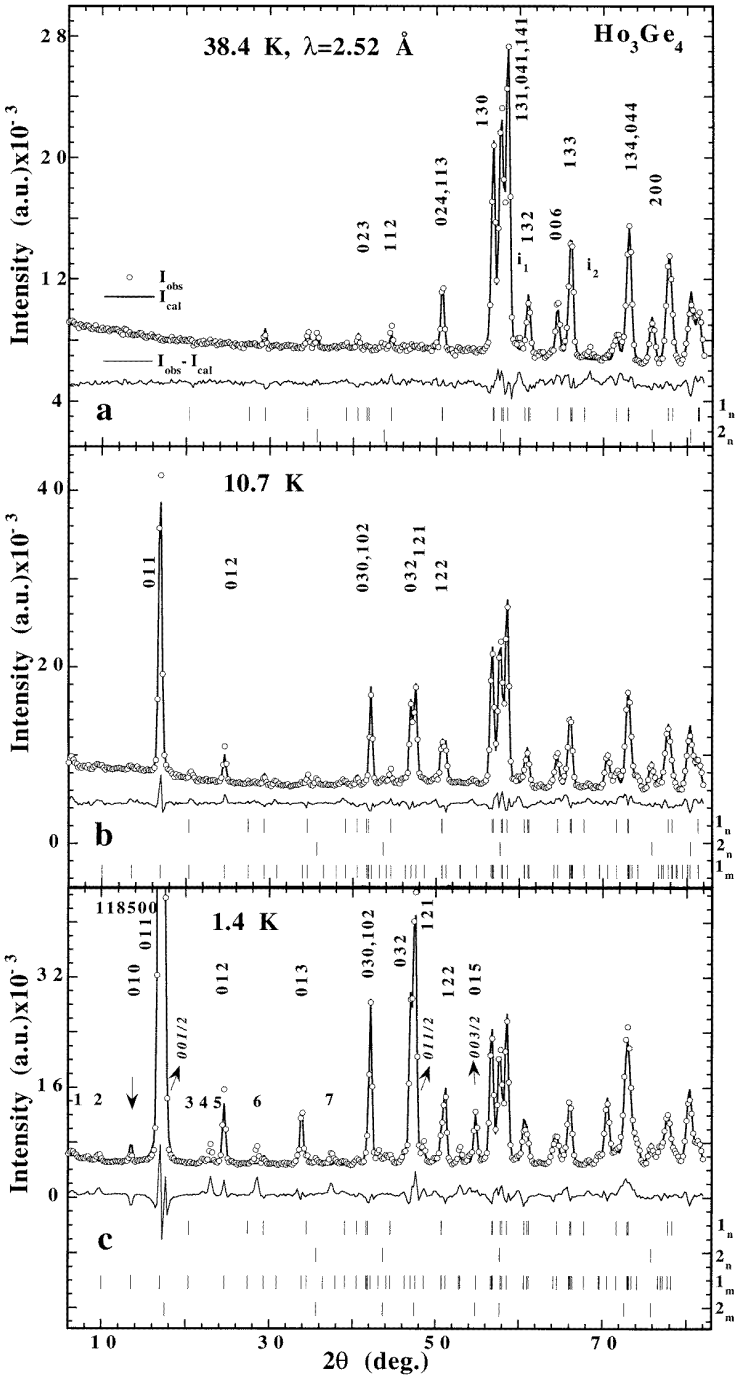

Figure 3. Observed, calculated and difference neutron diagram at 38.4 K (a), at 10.7 K (b) and 1.4 K (c). Four sets of reflections labelled by 1_n, 1_m, 2_n, 2_m in the right margin correspond to nuclear and magnetic contributions of Ho_3Ge_4 and $HoGe_{1.5}$, respectively. Main magnetic contributions of Ho_3Ge_4 are indexed in bold and of $HoGe_{1.5}$ in italic letters. Impurity lines are marked 1–7 in (c).

Table 2. Survey of ordering temperatures observed by neutron diffraction in several R_3Ge_4 compounds. T_N corresponds to the ordering of the R_1 moments and T_1 to that of the R_2 moments. For both sites also the preferred moment directions (PMD) have been listed.

	R = Tb	R = Dy	R = Ho	R = Er	R = Tm
T_N [K]	28	19	12	7.3	2.9
T_1 [K]	16.5	6	6.6	4	—
PMD site R_1	$\boldsymbol{a}$	$\boldsymbol{a}$	$\boldsymbol{c}$	$(0yz)$	b
PMD site R_2	$\boldsymbol{c}$	$\boldsymbol{c}$	$\boldsymbol{a}$	$\boldsymbol{c}$	$\boldsymbol{a}$

As will be shown in the next section this magnetic structure is only stable in the high-temperature region (HT, $T_N > T > T_1 = 6.6$ K).

4.3. The magnetic structure of Ho_3Ge_4 at 1.4 K

At temperatures below $T_1 = 6.6$ K (LT region) the topology and relative intensities of the magnetic reflections are modified compared to those at 10.7 K, as can be seen in figure 3(b), (c)). The most characteristic feature of the LT patterns is the appearance of the weak (010) line at $2\theta = 13.6^\circ$ and of the (013) line at $2\theta = 34.1^\circ$. These observations are compatible with an ordering of Ho_2 and/or a canting of the Ho_1 moments away from the $\boldsymbol{c}$-axis.

As no satisfactory solution could be found using the allowed modes of the HT magnetic space group, a symmetry lowering was considered in order to explain the observed intensities. The best fit of the observed magnetic intensities at 1.4 K was achieved assuming a uniaxial magnetic moment arrangement of the Ho_2 atoms at 4(c) along the $\boldsymbol{a}$-axis. This arrangement is described by the mode A_x–A_x $(+\,-\,-+)$ in the magnetic space group $Cp\frac{2'2'2_1}{mcm'}i'(\mathrm{Sh}_{63}^{453})$, the sign change pertains to the atoms ((1): $(0, y, 1/4)$, (2): $(0, -y, 3/4) + (1/2, 1/2, 0)$). No evidence of a moment reorientation of the Ho_1 sublattice is found.

The ordering of the two Ho sites is described by different magnetic space groups: Ho_1 has $Cp\frac{222_1}{m'c'm'}i'(\mathrm{Sh}_{52}^{318})$ symmetry, while Ho_2 $Cp\frac{2'2'2_1}{mcm'}i'(\mathrm{Sh}_{62}^{453})$. The resulting magnetic space group, being the intersection of the two individual groups has only monoclinic symmetry $Cp11\frac{2_1}{m'}i'(\mathrm{Sh}_{14}^{82})$. The total 1.4 K magnetic structure is displayed in figure 4.

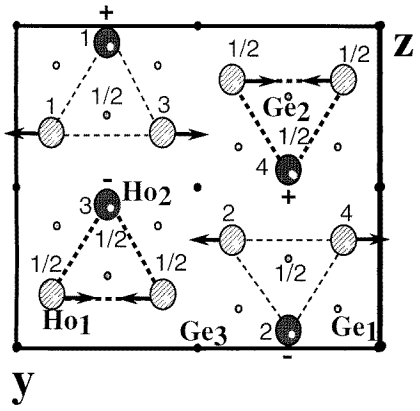

Figure 4. Projection of the low-temperature magnetic structure of Ho_3Ge_4 along the x-axis.

The refinement of the magnetic intensities at 1.4 K confirms the correctness of this model (figure 3(c), table 1). At 1.4 K the ordered moment values are $\mu_{2x} = 7.2(2)\ \mu_B$ for the Ho_2 site and $\mu_{1z} = 8.9(1)\ \mu_B$ for the Ho_1 site. These values are lower than the free-ion value of Ho^{3+} ($gJ\ [\mu_B] = 10\ [\mu_B]$).

4.4. Thermal evolution of magnetic ordering in Ho_3Ge_4

The thermal variation of some selected magnetic integrated intensities of Ho_3Ge_4 shown in figure 5 suggests the existence of two critical temperatures: $T_N = 12$ K and $T_1 = 6.6$ K. The transition temperatures are in agreement with the values obtained from the magnetization and specific heat measurements.

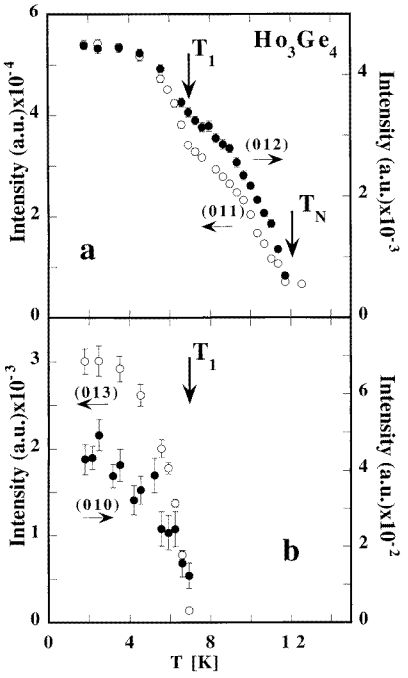

Figure 5. Temperature dependence of the magnetic intensities of the (011), (012) reflections (a) and (010), (013) reflections (b) of Ho_3Ge_4.

The (011) and (012) lines described in figure 5(a) arise at T_N due to the magnetic ordering of the Ho_1 sublattice. The temperature dependences of their intensities show a change in slope at T_1 when the magnetic ordering of the Ho_2 sublattice starts. The magnetic structure factors of the (011) and (012) reflections comprise contributions of both μ_{1z} and μ_{2x} magnetic moments which add up:

$$F(011) \sim 1.428\mu_{1z} + 0.945\mu_{2x} \tag{1}$$

$$F(012) \sim 0.931\mu_{1z} + 0.327\mu_{2x}. \tag{2}$$

The (010) and (013) lines described in figure 5(b) arise at T_1 and are associated with Ho_2 magnetic ordering. The magnetic structure factors of the (010) and (013) reflections are:

$$F(010) \sim 0.327\mu_{2x} \tag{3}$$

$$F(013) \sim 0.945\mu_{2x}. \tag{4}$$

The temperature dependences of μ_{1z} and μ_{2x} magnetic moments are presented in figure 6.

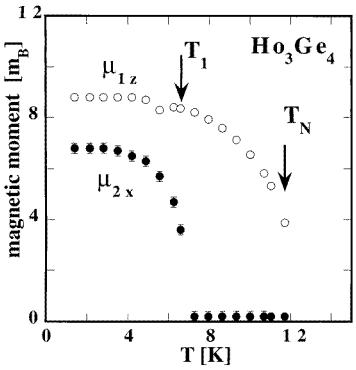

Figure 6. Thermal evolution of the magnetic moments μ_{1z} of Ho_1 and μ_{2x} of Ho_2 in Ho_3Ge_4.

Furthermore, in the temperature region 15–10 K the patterns comprise diffuse scattering in the vicinity of the (011) position. Most likely this appears due to short-range magnetic order near T_N and decreases with temperature lowering.

4.5. Secondary phases

In the paramagnetic regime foreign lines were detected in addition to the main contributions of the Ho_3Ge_4 phase. These lines were attributed to a phase with the AlB_2 structure (space group $P6/mmm$), as described in [7]. According to microspectral analysis (Camebax electron probe microanalyser, Ho Lα, Ge Kα lines, accelerating voltage of the electron beam 15 kV, sample current 40 mA) the composition of this phase is $HoGe_{2-\delta}$ ($\delta = 0.5$).

Below 10 K additional lines appear due to the antiferromagnetic ordering of the $HoGe_{1.5}$ phase with the wave vector $\boldsymbol{q} = (001/2)$. The topology and the relative intensities of the magnetic lines are similar to those observed in the isomorphic compounds $DyGe_{1.3}$ [2] and $TbGe_{1.5}$ [3]. Figure 7(a) displays the thermal evolution of the integrated intensity of the dominating (001/2) reflection, leading to an ordering temperature of $T_N = 10$ K. In the specific heat data this magnetic ordering shows up in the form of a small shoulder at the low-temperature side of the highest peak in the inset of figure 2.

A uniaxial antiferromagnetic arrangement ($+ - + - ..$) for the Ho atoms residing at the 1(a) position (000) gives quite satisfactory agreement between observed and calculated patterns at 1.4 K, as can be inferred from the results shown in figure 3(c) and table 1. The corresponding magnetic space group is $P_{2c}11\frac{2'}{m'}(\mathrm{Sh}_{11}^{56})$. At 1.4 K the ordered moment value is $\mu_{Ho} = 6.2(6)\ \mu_B$/Ho, and the preferred moment direction is perpendicular to the hexagonal axis.

As the amount of $HoGe_{1.5}$ does not exceed 22% a closer investigation of the crystal and magnetic structures on a single-phase sample is under way.

Furthermore for temperatures below 12 K some unidentified weak magnetic lines arise (marked 1–7 in figure 3(c)). These lines can be divided into three distinct sets according to their thermal behaviour which is different from that of the main phases: (a) 1 and 3, (b) 2 and 4, (c) 5, 6 and 7 (figure 7(b)). Most likely they pertain to the magnetic ordering

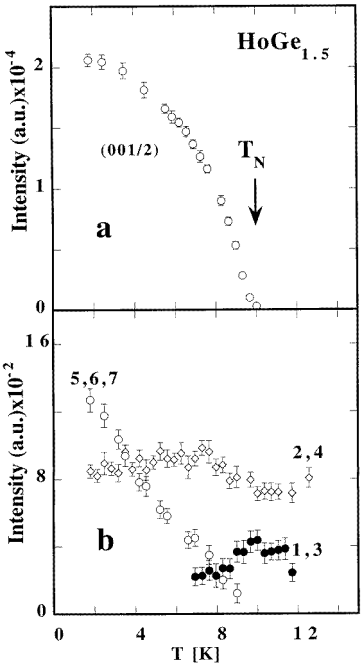

Figure 7. Temperature dependence of the (001/2) magnetic intensity of $HoGe_{1.5}$ (a) and of unidentified magnetic impurities 1–7 (b).

of other unknown $HoGe_x$ phase(s) occurring in this composition range, probably associated with the not-indexed nuclear lines i_1 and i_2 in the HT patterns, marked in figure 3(a).

5. Discussion

The evolution of magnetic order in Ho_3Ge_4 and the other three R_3Ge_4 compounds studied by us [1–3] displays some common features. With the exception of Er_3Ge_4 all examined compounds were found to display a two-step ordering of the moments associated with the two R sites. The two sublattice moments order independently with two distinct order parameters associated with the same wave vector $\boldsymbol{q} = (010)$. The 8(f) site moment orders below T_N while the 4(c) site moment does so only at substantially lower temperatures. Virtually the same behaviour is observed for the Dy_3Ge_4 and Tb_3Ge_4 compounds where the two sublattices have a uniaxial antiferromagnetic moment arrangement but with mutually perpendicular orientations.

The main differences in the magnetic ordering of the R_3Ge_4 series concerns the preferred direction of the magnetic moments. The easy axis of antiferromagnetism of the R_1 site moments lies along the $\boldsymbol{c}$-axis for Ho, along the $\boldsymbol{a}$-axis for Dy and Tb (for the latter in the HT region only), in the $(0yz)$ plane for Er and along the b-axis for Tm. The easy direction of the R_2 site moment is along the $\boldsymbol{a}$-axis of Ho and Tm and along the $\boldsymbol{c}$-axis for Er, Dy and Tb. A survey of the easy moment directions in the R_3Ge_4 compounds studied by us is given in table 2, including preliminary results obtained for Tm_3Ge_4 for which $g = (0\frac{1}{2}0)$ [8]. The easy moment directions listed for the R_1 site correspond to the situation close to T_N, where the moments of the R_1 atoms apparently order independently from those at the R_2 sites. From the values of T_N listed in table 2 it can be inferred that the magnetic

ordering of the R_1 moments scales to the de Gennes factor, $T_N \propto (g-1)^2 J(J+1)$. This means that the spin–spin coupling governing the intrasublattice interaction I_{11} and magnetic ordering of these moments is of the same type in all compounds, as can be expected for the conduction electron mediated RKKY type interaction.

When inspecting the easy moment direction listed in table 2 one has to consider that it depends essentially on the nature of the low-lying crystal field levels. The lowest-order term of the crystal field interaction is determined by the second-order Stevens factor α_J which is negative for Tb, Dy, Ho and positive for Er and Tm [9]. Inspection of the R_1 site easy moment direction listed in table 2 shows that there is a correlation with the sign of the second-order Stevens factor only for the site R_1. The R_3Ge_4 compounds for which α_J is negative (R = Tb, Dy, Ho) have an R_1 moment direction perpendicular to the $\boldsymbol{b}$-direction, whereas those with positive α_J have an R_1 moment direction parallel (R = Tm) or nearly parallel (R = E) to the $\boldsymbol{b}$-direction. It can also be derived from the data listed in table 2 that the easy moment directions do not correlate at all with α_J for site R_2, suggesting that the crystal field interaction plays only a minor role in determining the easy moment direction for this site. More importantly, it may be noticed that the easy moment directions for site R_2 tend to be perpendicular to those of site R_1, which tendency is most pronounced for Dy_3Ge_4, Ho_3Ge_4 and Tm_3Ge_4. At this moment it is useful to recall that the configuration of the atomic positions (as shown for example in figure 4) is a triangular one, and that the intersublattice and intrasublattice interactions are all antiferromagnetic. These facts suggest that the mutually perpendicular orientations of the moments at sites R_1 and R_2 arise as a consequence of geometric magnetic frustration [10]. This perpendicular moment arrangement and the concomitant absence or near absence of intersublattice interaction explains why the R_2 moments order independently from the R_1 moments. The R_2 moments order at a substantially lower temperature than the R_1 moments, meaning that $I_{22} < I_{11}$.

We mentioned already that at T_N only the R_1 moments become magnetically ordered and that the corresponding easy moment directions are determined by crystal field interactions. Depending on the relative strength of the crystal field induced anisotropy and the intersublattice coupling strength, the R_1 moments may deviate somewhat from their ideal easy direction. This is the case, for instance, in Tb_3Ge_4. Here the Tb_1 moments bend away from the $\boldsymbol{a}$-direction at T_N, to reach a more stable canted moment arrangement at lower temperatures, due to higher ordered moment values and the concomitant larger intersublattice interaction, the latter interaction becoming possible only for not strictly perpendicular R_1 and R_2 moments. Presumably, the crystal field induced anisotropy is relatively weak in the case of Er_3Ge_4 where the Er_1 moments bend away from the $\boldsymbol{b}$-direction already at T_N.

6. Conclusions

The magnetic structures and phase transitions of the novel phases Ho_3Ge_4 and $HoGe_{1.5}$ were studied by neutron diffraction, magnetic measurements and specific heat measurements.

A two-step antiferromagnetic ordering was found for Ho_3Ge_4. In the first step (below $T_N = 12$ K) the magnetic moments in the 8(f) Ho_1 site order in a simple uniaxial antiferromagnetic arrangement along the $\boldsymbol{c}$-axis.

In a second step (below $T_1 = 6.6$ K) the magnetic moments at the 4(c) Ho_2 site order antiferromagnetically. This arrangement is also uniaxial, but the moment direction is perpendicular to that of the Ho_1 atoms and lies along the $\boldsymbol{a}$-axis. This results in a two-dimensional canted antiferromagnetic structure and in lowering of the total symmetry.

We have compared the two-step antiferromagnetic ordering in Ho_3Ge_4 with similar types of magnetic ordering found in several other R_3Ge_4 compounds, and discussed the complex

ordering phenomena in these materials in terms of crystal field effects, antiferromagnetic intersublatice and intrasublattice interactions and the occurrence of magnetic frustration associated with the triangular atomic arrangement in the underlying crystal structure type.

Acknowledgment

This work is financially supported by the Swiss National Foundation, Bern.

References

[1] Schobinger-Papamantellos P, Oleksyn O, Ritter C, de Groot C H and Buschow K H J 1997 *J. Magn. Magn. Mater*. **169** 253
[2] Oleksyn O, Schobinger-Papamantellos P, Ritter C, de Groot C H and Buschow K H J 1997 *J. Alloys Compounds* **262–263** 492
[3] Oleksyn O, Schobinger-Papamantellos P, Ritter C, Janssen Y, Brück E and Buschow K H J 1997 *J. Phys.: Condens. Matter* **9** 1
[4] Ya Oleksyn O and Bodak O I 1994 *J. Alloys Compounds* **210** 19
[5] Rodriguez-Carvajal J 1993 *Physica* B **192** 55
[6] Bertaut E F 1963 *Magnetism* vol 3, ed G T Rado and H Suhl (New York: Academic) ch 4, p 149
Bertaut E F 1975 *Ann. Phys.* **9** 93
[7] Eremenko V N, Obushenko I M and Bujanov Yu I 1980 *Dopovidi Akad. Nauk Ukr. RSR* A **42** 91
[8] Zaharko O, Schobinger-Papamantellos P, Ritter C, Janssen Y, Brück E and Buschow K H J 1998 *J. Phys.: Condens. Matter* submitted
[9] Elliott R J (ed) 1972 *Magnetic Properties of Rare Earth Metals* (New York: Plenum)
[10] Schiffer P and Ramirez A P 1996 *Comment. Condens. Matter. Phys.* **18** 21